Characterization of Large-Pore MCM-41 Molecular Sieves Obtained via Hydrothermal Restructuring

A. Sayari and P. Liu

Department of Chemical Engineering and CERPIC Université Laval, Ste-Foy, Qc, Canada, G1K 7P4

M. Kruk and M. Jaroniec*

Department of Chemistry Kent State University, Ohio 44242

Received March 3, 1997. Revised Manuscript Received June 27, 1997[⊗]

MCM-41 periodic mesoporous silicates were synthesized using cetyltrimethylammonium bromide, and their pore sizes were tailored by postsynthesis hydrothermal treatment method of Khushalani et al., allowing us to obtain large-pore MCM-41 samples with a high degree of structural ordering. It was shown that the pore size enlargement was accompanied by a significant improvement of pore size uniformity, a gradual decrease of the specific surface area, and the pore wall thickening. After a certain upper limit of pore size (i.e., about 6.5 nm) was reached, a further hydrothermal treatment led to samples of diminished quality. The structural uniformity decreases dramatically, i.e., the pore size distribution becomes broader and a small but noticeable amount of micropores develops. Moreover, the appearance of pore blocking effects (as inferred from the irreversibility of nitrogen adsorption−desorption isotherms) indicates that the pore geometry deviates significantly from its initial cylindrical shape characteristic for MCM-41 materials. The current study confirmed previous findings that the hydrothermal restructuring method is a convenient way to synthesize high quality MCM-41 silicates with tailored pore sizes, but only up to 6.5 nm.

Introduction

Since the discovery of M41S family of periodic mesoporous materials,[1,2] a considerable effort was made in order to tailor their structures and properties. Most of the research in that field was devoted to MCM-41 silicate and aluminosilicate molecular sieves, which exhibit hexagonal arrays of cylindrical mesopores. Chemical properties of these materials were modified by framework incorporation of various heteroatoms, such as titanium, vanadium, and boron with the purpose of creating specific catalytic sites. Surface properties of MCM-41 molecular sieves were also changed by chemical bonding of organic groups. Moreover, the MCM-41 materials were used as hosts for organometallic complexes and as supports of oxides and metallic clusters. Progress in the field of chemical and surface modifications of ordered mesoporous materials was the subject of several recent reviews.[3−5]

Tailoring of the porous structure is another important issue in the design and application of MCM-41 materials. Such features as pore size,[1,2,6−9] pore size uniformity,[8,10] interparticle porosity,[11] and stability (thermal and hydrothermal)[12] of these mesoporous molecular sieves were shown to be controlled by a proper choice of synthesis conditions. The adjustment of pore sizes of MCM-41 molecular sieves was studied extensively during the early work carried out by scientists from Mobil R&D Corp.[1,2] They reported that the pore size of these materials increases with the chain length of the surfactant used in the synthesis. The use of quaternary ammonium surfactants $C_nH_{2n+1}(CH_3)_3NBr$ with n from 8 to 16 afforded samples of pore sizes in the range 1.8−3.8 nm, as determined on the basis of argon adsorption measurements.[2] Numerous later studies showed that pore sizes of MCM-41 materials obtained using various surfactants and synthesis procedures fall into the range between 1.5 and 4.5 nm.[5] Further pore size increase was attained by adding expander compounds, such as 1,3,5-trimethylbenzene (TMB)[13] or linear hydrocarbons.[14] Using such additives, materials with pores up to 8.5−12 nm in diameter were

* E-mail: Jaroniec@kentvm.kent.edu. Phone: (330) 672-3790. Fax: (330) 672-3816.

[⊗] Abstract published in *Advance ACS Abstracts,* August 15, 1997.

(1) Kresge, C. T.; Leonowicz, M. E.; Roth, W. J.; Vartuli, J. C.; Beck, J. S. *Nature* **1992**, *359*, 710.

(2) Beck, J. S.; Vartuli, J. C.; Roth, W. J.; Leonowicz, M. E.; Kresge, C. T.; Schmitt, K. D.; Chu, C. T.-W.; Olson, D. H.; Sheppard, E. W.; McCullen, S. B.; Higgins, J. B.; Schlenker, J. L. *J. Am. Chem. Soc.* **1992**, *114*, 10834.

(3) Sayari, A. *Chem. Mater.* **1996**, *8*, 1840.

(4) Sayari, A. In *Recent Advances and New Horizons in Zeolite Science and Technology*; Chon, H., Woo, S. I., Park, S.-E., Eds.; Elsevier: Amsterdam, 1996; Chapter 1.

(5) Raman, N. K.; Anderson, M. T.; Brinker, C. J. *Chem. Mater.* **1996**, *8*, 1682.

(6) Huo, Q.; Margolese, D. I.; Ciesla, U.; Feng, P.; Gier, T. E.; Sieger, P.; Leon, R.; Petroff, P. M.; Shüth, F.; Stucky, G. D. *Chem. Mater.* **1994**, *6*, 1176.

(7) Kruk, M.; Jaroniec, M.; Sayari, A. *J. Phys. Chem. B* **1997**, *101*, 583.

(8) Huo, Q.; Margolese, D. I.; Stucky, G. D. *Chem. Mater.* **1996**, *8*, 1147.

(9) Khushalani, D.; Kuperman, A.; Ozin, G. A.; Tanaka, K.; Garces, J.; Olken, J. J.; Coombs, N. *Adv. Mater.* **1995**, *7*, 842.

(10) Kruk, M.; Jaroniec, M.; Ryoo, R.; Kim, J. M. *Microporous Mater.*, in press.

(11) Tanev, P. T.; Pinnavaia, T. J. *Science* **1995**, *267*, 865.

(12) Ryoo, R.; Kim, J. M.; Ko, C. H.; Shin, C. H. *J. Phys. Chem. B* **1997**, *101*, 317.

(13) Beck, J. S. U.S. Patent 5,057,296, 1991.

(14) Ulagappan, N.; Rao, C. N. R. *Chem. Commun.* **1996**, 2759.

S0897-4756(97)00128-2 CCC: $14.00

obtained,[2] but the uniformity of the porous structures was found to be inferior in comparison with samples of small pores (i.e., about 3−4 nm in diameter).[8]

To obtain high-quality-large pore MCM-41 samples, new synthesis approaches based on postsynthesis hydrothermal treatment of samples prepared in a conventional manner[8,9] were developed. Khushalani et al.[9] reported that when a conventional synthesis of MCM-41 materials carried out at low temperature (343 K) is followed by a hydrothermal treatment of the samples at 423 K in their mother liquor for a period of 1−10 days, a gradual pore size expansion up to ca. 7 nm takes place. As inferred from their XRD and pore size distribution data, the quality of the samples improved gradually during the first 3−5 days. The authors suggested that the thermal restructuring process involves silica dissolution, transport, and redeposition in areas with high surface curvature. Similarly, Huo et al.[8] found that MCM-41 materials prepared in the presence of a mixture of a divalent surfactant with a gemini or an alkyltrimethylammonium surfactant and subsequently washed and dried can be subjected to a mild hydrothermal treatment in water at 373 K in order to obtain high-quality materials with pore sizes up to ca. 6 nm.

The aim of the current study was (i) to synthesize a series of MCM-41 molecular sieves with a wide range of pore sizes via postsynthesis hydrothermal treatment,[9] and (ii) to characterize their pore structure using nitrogen adsorption over a wide range of pressures.

Experimental Section

Materials. All samples were prepared in the presence of cetyltrimethylammonium bromide (CTAB) using the same gel composition as Khushalani et al.,[9] i.e., 1 SiO_2:0.33 TMAOH: 0.17 CTAB:0.17 NH_4OH:17 H_2O. The following is a typical preparation procedure. Cab-O-Sil M-5 silica (3.6 g) was suspended in water (6 g) under vigorous stirring, and then 6.16 g of 25 wt % tetramethylammonium hydroxide (TMAOH) was added. Independently, 3.65 g of CTAB was dissolved in 6.56 g of water, and subsequently 1.17 g of 30 wt % NH_4OH was introduced. The mixtures containing the silica and CTAB were stirred together for ca. 30 min, then transferred into a Teflon-lined autoclave, and treated under autogenous pressure without stirring at 343 K for 3 days. For further postsynthesis thermal treatment, the autoclave was transferred in another oven and heated for an additional period of time at a desired higher temperature. Then, the sample was filtrated, washed, dried, and calcined at 540 °C for 5 h under flowing air (6 L/h).

During the course of this study four sets of samples were prepared. For the first three series of samples, the postsynthesis treatment temperature was carried out at 423 K. The following notation is used for these samples. The "mother" sample, which was not treated hydrothermally, is denoted as BTR. The thermally restructured samples are designated as TR*n*−*t*, where *n* specifies the number of a series of samples, to which a given sample belongs, and *t* indicates the time in days (d) or hours (h) of hydrothermal treatment at 423 K. For example, TR1−3d is a material from the first group of samples, which was hydrothermally restructured for 3 days at 423 K. The fourth series consisted of three samples that were treated for 2 days at temperatures of 393, 403, and 413 K. In this case, the temperature will be explicitly shown in their symbols, e.g., TR393K is the sample treated hydrothermally at 393 K for 2 days.

Measurements. X-ray powder diffraction (XRD) spectra were recorded on a Siemens D5000 diffractometer using a nickel-filtered Kα radiation. Nitrogen adsorption−desorption measurements were performed using a volumetric adsorption analyzer ASAP 2010 manufactured by Micromeritics, Norcross, GA. The samples under study were degassed for 2 h at 473 K, and subsequently the measurements were carried out at 77 K over a wide relative pressure range from ca. 10^{-6} to 0.995.

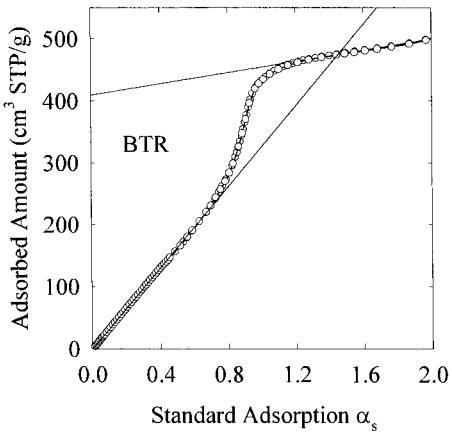

Figure 1. High-resolution α_s-plot for the "mother sample" (BTR), which was not hydrothermally treated.

Calculation Methods. The BET specific surface area S_{BET} was calculated using the standard BET method[15] for adsorption data in a relative pressure range from 0.04 to 0.2. The total surface area S_t, the primary mesopore volume V_p, the micropore volume V_{mi}, and the external surface area S_{ex} were obtained using the high-resolution α_s-plot method.[10,16−18] Li-Chrospher Si-1000 silica gel (S_{BET} = 25 m^2/g) was used as a reference adsorbent. It needs to be noted that according to IUPAC recommendations,[19] pores are classified as micropores (width below 2 nm), mesopores (width between 2 and 50 nm) and macropores (width greater than 50 nm). Moreover, in the current study, intracrystalline cylindrical pores of MCM-41 materials are referred to as primary mesopores, whereas other mesopores present in the samples are called secondary mesopores. The total surface area S_t is defined as the surface area of mesopores and macropores. When microporosity is not present, as is the case for most MCM-41 molecular sieves, S_t provides the specific surface area for a given material. The external surface area S_{ex} is defined as the surface area of macropores and secondary mesopores.

In the α_s-plot method, the adsorption isotherm $v(p)$ on a porous solid under study is transformed from a function of the equilibrium pressure p to a function of the amount adsorbed on the reference material. The latter adsorbed amount is usually written as the reduced standard adsorption: $\alpha_s = v_{ref}(p)/v_{ref,0.4}$, where $v_{ref}(p)$ is the amount adsorbed on the reference solid as a function of the equilibrium pressure p, and $v_{ref,\,0.4}$ is the amount adsorbed at the relative pressure $p/p_0 = 0.4$. To express the adsorption isotherm $v(p)$ for a given sample as a function of α_s, i.e., as $v(\alpha_s)$, the α_s values corresponding to given pressure values are obtained from the adsorption isotherm $v_{ref}(p)$ for the reference adsorbent. Illustrative α_s-plots are shown in Figures 1−4. The presence of linear segments on the α_s-plot curves indicate that in the corresponding pressure range the course of adsorption on a given sample is essentially the same as the course of adsorption for the nonporous reference adsorbent. The slope of such linear segments can be used to calculate the surface area of the sample or the surface area of a certain group of pores within the sample. The intercept with the "adsorbed amount" axis of the plot provides the amount adsorbed in a certain group of pores and thus, their volume. These general concepts of the α_s-plot method can be used in

(15) Brunauer, S.; Emmett, P. H.; Teller, E. *J. Am. Chem. Soc.* **1938**, *60*, 309.
(16) Gregg, S. J.; Sing, K. S. W. *Adsorption, Surface Area and Porosity*; Academic Press: London, 1982.
(17) Kaneko, K.; Ishii, C.; Ruike, M.; Kuwabara, H. *Carbon* **1992**, *30*, 1075.
(18) Kruk, M.; Jaroniec, M.; Choma, J. *Carbon*, in press.
(19) Sing, K. S. W.; Everett, D. H.; Haul, R. A. W.; Moscou, L.; Pierotti, R. A.; Rouquerol, J.; Siemieniewska, T. *Pure Appl. Chem.* **1985**, *57*, 603.

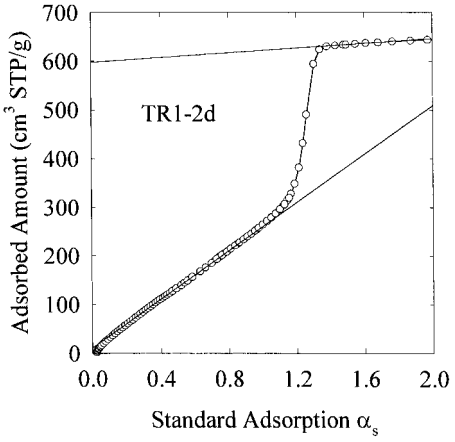

Figure 2. High-resolution α_s-plot for the TR1−2d sample indicating the presence of microporosity.

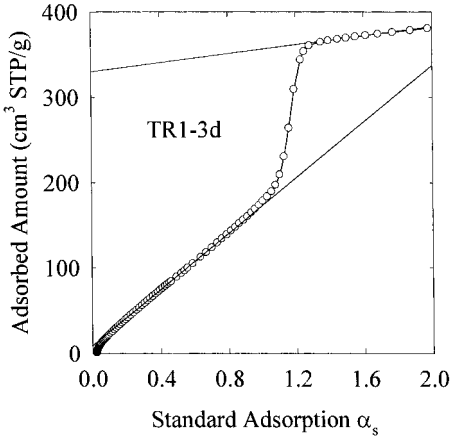

Figure 3. High-resolution α_s-plot for the TR1−3d sample indicating the presence of microporosity.

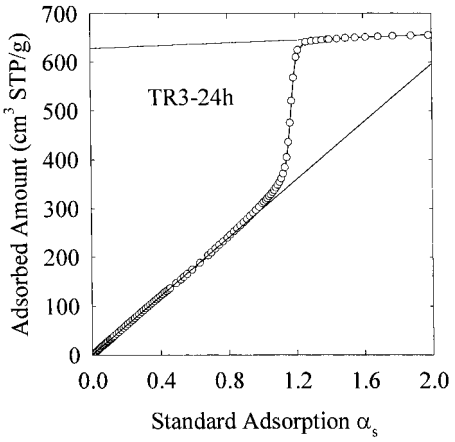

Figure 4. High-resolution α_s-plot for the large pore TR3−24h sample.

studies of novel ordered mesoporous materials in the way described below.

The adsorption data in a low-pressure range can be used to assess the total surface area S_t and the micropore volume V_{mi} on the basis of the following formula:

$$v = v_{mi} + \eta_1 \alpha_s \qquad for\ \alpha_{s,mi} < \alpha_s < \alpha_{s,pm1} \tag{1}$$

where η_1 and v_{mi} are, respectively, the slope of the line drawn through the linear part of the α_s-plot and its intercept with the "adsorbed amount" axis. The lower limit $\alpha_{s,\,mi}$ of the α_s values used in these calculations corresponds to the relative pressure, for which micropores possibly present in the sample are completely filled by the adsorbate. When there are no micropores in a given sample, $\alpha_{s,mi}$ can be set to zero. Moreover, the upper limit ($\alpha_{s,\,pm1}$) needs also to be imposed in order to exclude data from the pressure range, in which the condensation in primary mesopores start to take place. Usually, an $\alpha_{s,\,pm1}$ of 0.7 is suitable, unless one performs calculations for samples with very small mesopores of about 2 nm in diameter. The intercept v_{mi} provides the amount adsorbed in micropores and can be used to calculate the micropore volume $V_{mi} = v_{mi}\, c_f$, where c_f is a conversion factor between the volume of gas and liquid adsorbate (when V_{mi} and v_{mi} are expressed in cm³/g and cm³ STP/g, respectively, c_f = 0.001 54 68 for nitrogen adsorbate at 77 K). The slope η_1 is related to the total surface area (defined above) for the sample: $S_t = \eta_1 S_{BET,ref}/v_{0.4,ref}$, where $S_{BET,\,ref}$ and $v_{0.4,ref}$ are the BET specific surface area and the amount adsorbed at $p/p_0 = 0.4$ for the reference adsorbent.

High-pressure adsorption data (α_s above ca. 1.2, which corresponds to $p/p_0 > 0.6$) can be used to assess the external surface area S_{ex} and the primary mesopore volume V_p for the samples based on the following formula:

$$v = v_p + \eta_2 \alpha_s \qquad for\ \alpha_{s,pm2} < \alpha_s < \alpha_{s,sm} \tag{2}$$

where η_2 and v_p are, respectively, the slope and the intercept of the line drawn through the high-pressure linear part of the α_s-plot toward the "adsorbed amount" axis. The α_s values used for these calculations should be greater than $\alpha_{s,\,pm2}$ value, which corresponds to the upper limit of the range of relative pressures, for which the condensation in the primary mesopores of the sample takes place. Moreover, an upper limit of the α_s values , i.e., $\alpha_{s,sm}$, should be imposed in order to exclude data for pressures, for which the capillary condensation in secondary mesopores occurs. The intercept v_p is related to the primary mesopore volume: $V_p = v_p\, c_f - V_{mi}$, and since most MCM-41 samples do not show any evidence of microporosity, the simplified formula $V_p = v_p\, c_f$ can be used. The external surface area can be obtained from the slope η_2 of the α_s-plot: $S_{ex} = \eta_2 S_{BET,ref}/v_{0.4,ref}$. The primary mesopore surface area S_p is calculated as a difference between the total surface area and the external surface area: $S_p = S_t - S_{ex}$. Note that the validity of eqs 1 and 2 rests upon the assumption that after condensation of the adsorbate in a certain group of pores (i.e., micropores or primary mesopores), the amount adsorbed in them remains essentially constant despite the further pressure increase.

The total pore volume V_t for the samples under study was assessed from a single point adsorption at a relative pressure of 0.99 ($v_{0.99}$) by converting the volume of the adsorbed gas to the volume of the liquid adsorbate: $V_t = v_{0.99} c_f$. The primary mesopore diameter w_d was calculated from the d_{100} X-ray spacing (later denoted as d spacing) and the specific primary mesopore volume V_p using the following relation:[7,20]

$$w_d = cd\left(\frac{\rho V_p}{1 + \rho V_p}\right)^{1/2} \tag{3}$$

where $c = (8/(3^{1/2}\pi))^{1/2} = 1.213$ and $\rho = 2.2$ g/cm³ was used as the density of pore walls.[21] Equation 3 is valid for materials with structures, that can be approximated as an infinite array of cylindrical pores arranged in a hexagonal pattern and therefore is suitable for MCM-41 molecular sieves. The primary mesopore diameter $w_{4V/S}$ was also assessed from the primary mesopore surface area S_p and primary mesopore volume V_p assuming a cylindrical pore geometry: $w_{4V/S} = 4V_p/S_p$,[7,22] but the latter method seems to be less accurate than the former.[7]

(20) Dabadie, T.; Ayral, A.; Guizard, C.; Cot, L.; Lacan, P. *J. Mater. Chem.* **1996**, *6*, 1789.
(21) Marler, B.; Oberhagemann, U.; Vortmann, S.; Gies, H. *Microporous Mater.* **1996**, *6*, 375.
(22) Franke, O.; Schulz-Ekloff, G.; Rathousky, J.; Starek, J.; Zukal, A. *J. Chem. Soc., Chem. Commun.* **1993**, 724.

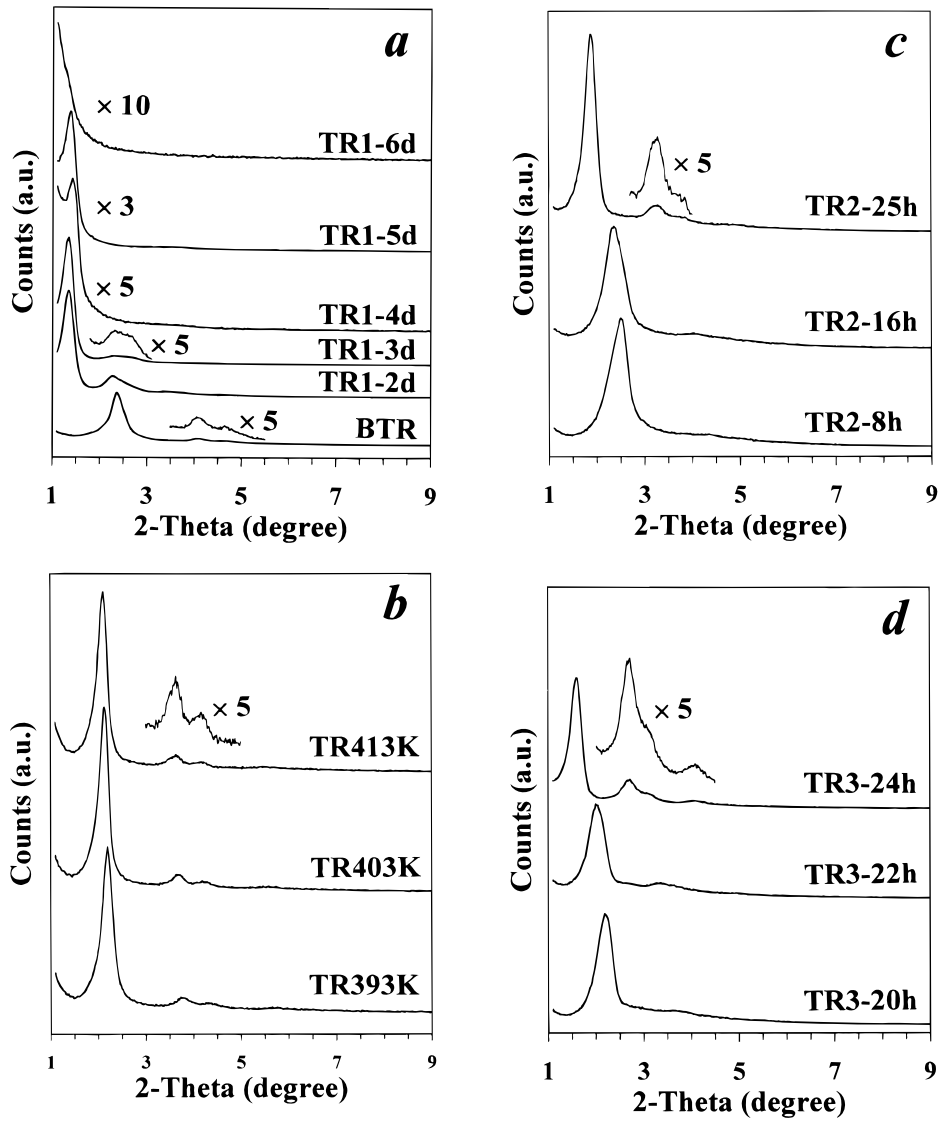

Figure 5. X-ray diffraction spectra for (a) samples from TR1 series, (b) samples treated at temperature below 423 K, (c) samples from TR2 series, and (d) samples from TR3 series. See text for an explanation of the notation used.

Table 1. Interplanar Spacing, Pore Center Distance and BET Specific Surface Area for the Samples Studied

sample	interplanar spacing d_{100} (nm)	pore center distance a (nm)	BET specific surface area S_{BET} (m^2/g)
BTR	3.72	4.30	1040
TR1−2d	6.59	7.61	770
TR1−3d	6.59	7.61	520
TR1−4d	6.2	7.2	170
TR1−5d	6.4	7.4	120
TR1−6d			25
TR2−25h	4.69	5.42	990
TR3−24h	5.52	6.37	890
TR3−22h	4.41	5.09	1010
TR3−20h	4.05	4.68	1070

3. Results and Discussion

The X-ray diffraction spectra for the four series of samples are shown in Figure 5. As seen in Table 1, the interplanar spacing d_{100} for the calcined "mother sample" BTR, which did not undergo any postsynthesis hydrothermal treatment, is equal to 3.72 nm, which is typical for MCM-41 silicates synthesized using cetyltrimethylammonium bromide as a templating surfactant. For the first series of samples, the same conditions of the hydrothermal treatment were used as in the work of Khushalani et al.[9] However, the d spacing increase occurred much faster than was reported in the literature. It took only 2 days of treatment at 423 K for the d spacing to increase from 3.72 to its maximum value of about 6.6 nm (see Figure 5a and Table 1).

The nitrogen adsorption isotherm for the BTR material, which was prepared at relatively low temperature and was not subject to the hydrothermal restructuring, is shown in Figure 6. It can be noticed that the sample exhibits a rather low degree of structural ordering. The step corresponding to nitrogen condensation in primary mesopores is broad, and there is a pronounced high-pressure hysteresis loop indicating the presence of a considerable amount of secondary mesopores. The BET specific surface area S_{BET}, the primary mesopore volume V_p, and the primary mesopore diameter w_d for the BTR sample were estimated as 1040 m^2/g, 0.63 cm^3/g, and 3.44 nm, respectively.

After 2 days of postsynthesis hydrothermal treatment, the properties of the sample changed dramatically. The main XRD peak became more pronounced (Figure 5a), the interplanar d spacing increased to 6.59 nm, the primary mesopore volume increased to 0.91 cm^3/g, while the BET specific surface area decreased to 770 m^2/g. As can be seen from the adsorption isotherm for the TR1−

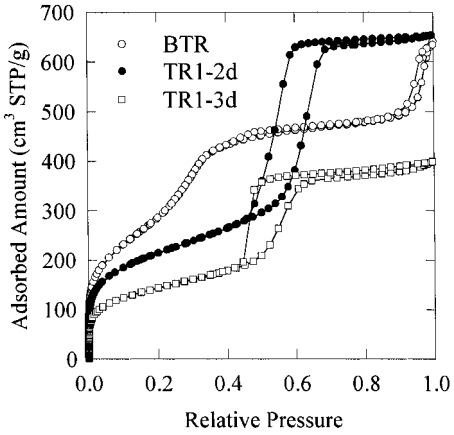

Figure 6. Nitrogen adsorption isotherms for BTR, TR1−2d, and TR1−3d samples.

Table 2. Structural Parameters for Selected Samples under Study

sample	BET specific surface area (m^2/g)	external surface area (m^2/g)	primary mesopore vol (cm^3/g)	total pore vol (cm^3/g)	relative pressure of nitrogen condensation p_c/p_0
TR393K	1400	30	0.72	0.77	∼0.23
TR403K	1280	40	0.74	0.78	∼0.26
TR413K	1200	50	0.73	0.77	∼0.27
TR2−16h	1200	40	0.80	0.85	∼0.30
TR2−8h	1240	30	0.79	0.83	∼0.28

2d sample (Figure 6), the nitrogen condensation takes place at much higher relative pressures (e.g., about 0.63) than in the case of the BTR MCM-41 material, which indicates a significant pore size enlargement. The primary mesopore diameter w_d for the TR1−2d material was estimated as 6.53 nm. In contrast to the adsorption behavior of the BTR sample, the nitrogen condensation in the primary mesopores of the hydrothermally restructured material is irreversible, i.e., accompanied by a pronounced hysteresis loop for relative pressures between 0.4 and 0.7. It is worth mentioning that similarly to previous studies,[8,9] it was found that the thermally restructured materials exhibit a relatively small decrease in the interplanar spacing upon calcination. For example, the *d* spacing of the BTR sample decreased from 4.33 to 3.72 nm (i.e., 14%), while TR1−2d underwent only 4.5% shrinkage.

The further hydrothermal treatment led to a gradual degradation of the porous structure of the materials. The TR1−3d sample, which underwent thermal restructuring for 3 days, exhibited a similar XRD pattern as TR1−2d, in terms of both peak intensity and *d* spacing (Figure 5a) and yet it suffered a significant decrease in the primary mesopore size, volume and surface area (see Tables 1−3). Note also that the corresponding adsorption−desorption isotherm had a very broad hysteresis loop. This excessive broadening of the hysteresis loop most probably arises from a gradual loss of pore diameter uniformity along the cylindrical pores in the structure of the material. Most likely, narrower parts within the pores developed and their presence caused connectivity problems during the desorption process,[23] which led to the broad hysteresis loop.

When the hydrothermal restructuring at 423 K was carried out for more than 3 days, the obtained materials had highly nonuniform porous structures, which manifested itself in a significant decrease in the specific surface area and pore volume (see Tables 1 and 3). Moreover, there was a gradual weakening of the (100) XRD peak and the disappearance of the (110) and (200) peaks (TR1−4d and TR1−5d), which eventually led to a featureless spectrum (see the XRD spectrum for TR1−6d in Figure 5a). Moreover, as can be seen in Figure 7, the adsorption−desorption isotherms for TR1−4d, TR1−5d, and TR1−6d did not close, even at low relative pressures. It occurred that using our adsorption apparatus, it was not possible to attain pressures low enough for the desorption branch of the isotherm to reach the adsorption branch. During the nitrogen desorption run for the TR1−4d sample, after the relative pressure of 0.003 was attained, it was extremely difficult to obtain the next experimental point for lower pressures due to an exceptionally slow equilibration. More than 12 h would be required to reach the equilibrium during that measurement, in comparison to a usual equilibration time of ca. 0.5 h for a single point on an adsorption−desorption isotherm. However, consecutive adsorption measurements on these low surface area samples were reproducible, which indicated that their structure was not appreciably altered in the course of the measurements.

Table 3. Structural Parameters Obtained from the High Resolution α_s-Plot Method for the Samples under Study

sample	total surface area (m^2/g)	external surface area (m^2/g)	primary mesopore surface area (m^2/g)	primary mesopore volume (cm^3/g)	total pore volume (cm^3/g)
BTR	940	130	810	0.63	0.97
TR1−2d	720[a]	60	660	0.91[c]	1.01
TR1−3d	470[a]	80	390	0.50[c]	0.62
TR1−4d	160[a]	40	120	0.04[c]	0.29
TR1−5d	120	*b*	*b*	*b*	0.13
TR1−6d	25	*b*	*b*	*b*	0.04
TR2−25h	950	30	920	0.88	0.92
TR3−24h	860	40	820	0.97	1.02
TR3−22h	950	30	920	0.81	0.86
TR3−20h	990	20	970	0.78	0.81

[a] The α_s-plots for these samples indicated the presence of some microporosity (the micropore volume V_{mi} is equal to ca. 0.02 cm^3/g for both TR1−2d and TR1−3d, and ca. 0.01 cm^3/g for TR1−4d), so the total surface area for such samples provides the surface area of the mesopores and macropores only (whereas the surface area of micropores is not included). [b] Not estimated due to the lack of a linear high-pressure part of the α_s-plot. [c] Correction for the micropore volume was introduced.

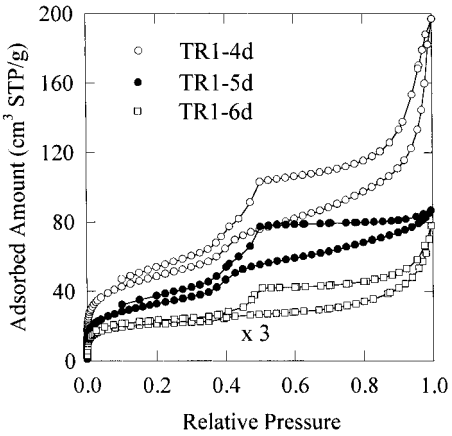

Figure 7. Nitrogen adsorption isotherms of the samples treated hydrothermally for long periods of time (4−6 days).

(23) Liu, H.; Zhang, L.; Seaton, N. A. *J. Colloid Interface Sci.* **1993**, *156*, 285.

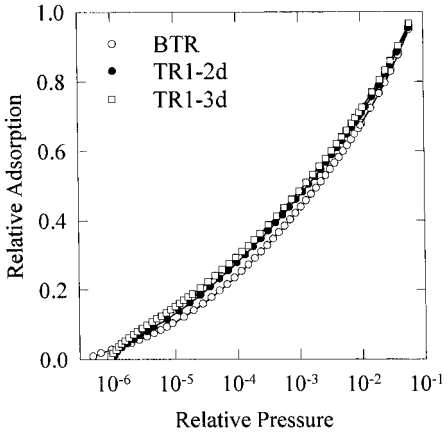

Figure 8. Relative adsorption curves for the nonrestructured sample and samples restructured at 423 K for 2 and 3 days.

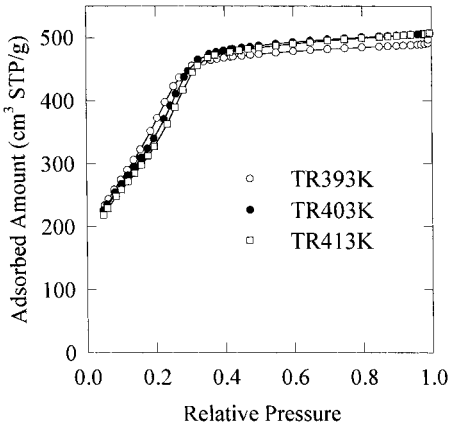

Figure 9. Nitrogen adsorption isotherms for samples treated hydrothermally at temperatures lower than 423 K.

Most likely, the observed adsorption−desorption irreversibility arises exclusively from network effects. It was shown by means of transmission electron microscopy[9] that during the hydrothermal restructuring process, the pore size becomes nonuniform, the shape of pores loses its regularity and some parts of pore walls are broken. Our adsorption studies confirm the appearance of defects in the pore walls of the samples. As can be seen in Figure 8, the relative adsorption curve (the relative adsorption is equal to the amount adsorbed for a given sample divided by its monolayer capacity calculated from the α_s-plot method) for the nonrestructured BTR sample initially rises rather slowly and gradually. In contrast, the curves for the samples treated hydrothermally for 2 and 3 days (TR1−2d and TR1−3d) exhibited much more pronounced initial increase, which might indicate the presence of microporosity. The high-resolution α_s-plot method provided a strong evidence of the presence of small amounts of micropores. As can be seen in Figure 1, the low-pressure part of the α_s-plot for the BTR sample is linear and passes through the origin of the graph, which shows the lack of microporosity. However, the α_s-plots for restructured samples TR1−2d and TR1−3d (Figures 2 and 3) are bent downward at very low relative pressures, i.e., α_s values close to 0. The latter finding indicates the presence of small but measurable amounts of micropores. It can be speculated that the latter are holes in the broken pore walls observed previously,[9] which is also supported by the fact that for samples treated hydrothermally for longer than 3 days, the microporosity gradually disappeared. That can be explained when one assumes that the defects in pore walls grow and eventually exceed the micropore size range.

Recently, pore blocking effects during adsorption−desorption in slitlike pores with narrow mouths were studied by means of computer simulations,[24] and the obtained adsorption isotherms appeared to be very similar to those reported in the current study for the TR1−4d, TR1−5d, and TR1−6d samples. This similarity additionally supports the idea that the adsorption−desorption irreversibility down to low relative pressures originates from considerable heterogeneity of pore diameters along the originally cylindrical pores of these restructured MCM-41 materials. It also needs to be noted that a similar shape of the adsorption−desorption isotherm was reported for the SBA-2 sample,[25] which was shown to exhibit a 3-dimensional structure of a hexagonal $P6_3/mmc$ symmetry with regular mesopore cages and a high surface area. In the case of the latter material, such a shape of the adsorption−desorption isotherm can be attributed to the fact that junctions between cages are much narrower than the cages themselves,[25] which causes connectivity problems upon nitrogen desorption.[23,24] Namely, the nitrogen condensed in cages cannot desorb until the desorption pressure for the pore mouths is reached[23] or the region of spinodal decomposition of nitrogen condensed in the cages is achieved.[24] It is possible that the materials obtained in the current study after 4 or more days of hydrothermal treatment exhibit an irregular structure of 3-dimensional cages of nonuniform size and rather random connectivity between the cages.

It is interesting to notice that the time scale of the hydrothermal restructuring observed in the current work is much shorter than was reported previously,[9] although similar conditions were used. The reaction appeared to be extremely sensitive to temperature and possibly to other more subtle variables. As can be seen from their XRD patterns (Figure 5b), there was no significant structural changes between samples hydrothermally treated at 393, 403, or even at 413 K for 2 days. This is also consistent with the N_2 adsorption data shown in Figure 9. However, closer examination of Figure 9 reveals that there are some slight differences in pore size. The relative pressure of nitrogen condensation in primary mesopores of the samples increases with the treatment temperature, indicating that the TR393K has the lowest and TR413K the highest pore size.

As discussed earlier, the TR1−2d sample showed some evidence of structural degradation, suggesting that the hydrothermal treatment applied was already too long. Therefore, two new series of samples were synthesized applying shorter times of hydrothermal restructuring. The structural and adsorption data for these samples are listed in Tables 1-4. The corresponding XRD spectra are displayed in Figure 5c,d, and the

(24) Maddox, M. W.; Lastoskie, C. M.; Quirke, N.; Gubbins, K. E. In *Fundamentals in Adsorption*; LeVan, M. D., Ed.; Kluwer: Boston, 1996; p 571.

(25) Huo, Q.; Leon, R.; Petroff, P. M.; Stucky, G. D. *Science* **1995**, *268*, 1324.

Table 4. Relative Pressure of Nitrogen Condensation in Primary Mesopores, Primary Mesopore Diameter and Pore Wall Thickness for the Samples

sample	relative pressure of nitrogen condensation p_c/p_0	pore width[a] w_d (nm)	pore wall thickness b_d (nm)	pore width $w_{4v/s}$ (nm)
BTR	~0.29	3.44	0.86	3.12
TR1−2d	~0.63	6.53	1.08	5.58
TR1−3d	~0.55	5.77	1.84	5.00
TR1−4d	~0.40			
TR1−5d	~0.40			
TR1−6d	~0.39			
TR2−25h	~0.43	4.62	0.80	3.83
TR3−24h	~0.57	5.53	0.84	4.76
TR3−22h	~0.41	4.28	0.81	3.54
TR3−20h	~0.34	3.90	0.78	3.22

[a] Calculated from XRD *d*-spacing and primary mesopore volume using eq 4.

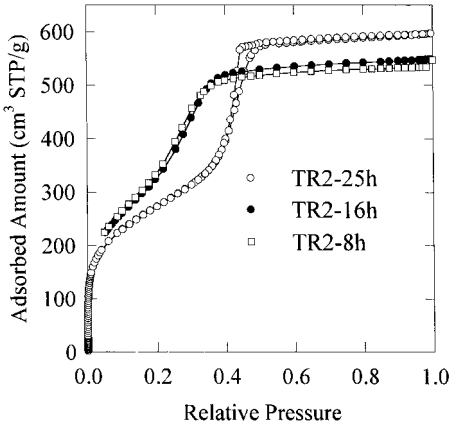

Figure 10. Nitrogen adsorption isotherms showing structural changes in the materials restructured at 423 K for 8−25 h (TR2 series).

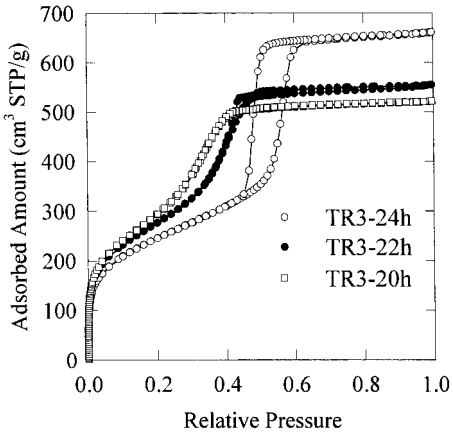

Figure 11. Nitrogen adsorption isotherms for a series of samples restructured at 423 K for 20−24 h (TR3 series).

adsorption isotherms and relative adsorption curves are shown in Figures 10−12. It can be noticed that the restructuring process has a rather unusual kinetics. There are no significant structural differences between samples treated at 423 K for 8 and 16 h, since there is only a slight increase in the pore volume and pore size, as judged from relative pressures corresponding to the nitrogen condensation in primary mesopores. However, there was a remarkable structural change taking place during the next 9 h of the hydrothermal treatment. The primary mesopore volume and the pore size increased considerably. Moreover, the main XRD peak became sharper and the smaller (110), (200), and (210) peaks

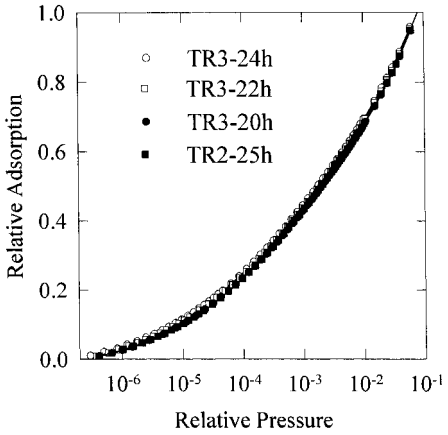

Figure 12. Relative adsorption curves for the samples which underwent pore size increase without degradation of their porous structures.

became more pronounced. As can be seen from the X-ray pattern for the TR2−25h sample (Figure 5c) and its nitrogen adsorption isotherm (Figure 9), this sample exhibits a high degree of structural uniformity as manifested in the occurrence of four distinct XRD peaks and a sharp step of nitrogen condensation in primary mesopores. Moreover, the α_s-plot for the sample (not shown) does not provide any evidence of microporosity, which indicates that degradation of the pore wall structure did not take place.

Another series of samples (TR3−20h, TR3−22h, and TR3−24h) was thermally treated for periods of time between 20 and 24 h. Gradual structure changes took place. The pore volume and the pore size increased and both total and primary mesopore surface areas decreased with time of the hydrothermal treatment (see Tables 3 and 4). In addition, as in the TR2 series, the XRD peaks become sharper and clearer (Figure 5d). As can be seen from the XRD spectrum (Figure 5d) and adsorption isotherm (Figure 11), the TR3−24h exhibits a remarkable structural uniformity, high primary mesopore volume (0.97 cm^3/g), and large pore size of 5.5 nm. The relative adsorption curve (Figure 12) and the high-resolution α_s-plot for this sample (Figure 4) indicate the absence of microporosity. It needs to be noted that the synthesis method is not strictly reproducible. For example, the sample structurally similar to previously described TR2−25h was TR3−22h, which underwent a hydrothermal treatment during only 22 h. Another example is that TR3−24h exhibited larger pores than TR2−25h even though its hydrothermal treatment was 1 h shorter. Nevertheless, it is clear that at 423 K there is an induction period of 15−20 h during which there is some decrease in the external and primary mesopore surface areas, but the actual pore enlargement takes place afterward.

The obtained results provide many details about the hydrothermal restructuring process. This process proved to be extremely sensitive to both the temperature and the time of postsynthesis treatment. Important changes occur even before an expansion of the unit cell of the material can be observed. For example, the treatment at low temperature (e.g., 393 K), or for short periods of time (e.g., 8 or 16 h at 423 K) brings about an initial marked decrease in the external surface area of the samples, since S_{ex} is equal to 130 m^2/g for the "mother sample" BTR but decreases to about 30−50 m^2/g. This

is paralleled by a decrease in the primary mesopore surface area (Table 2). In a second step, a pore size enlargement accompanied by an increase in the pore size uniformity and a decrease in the surface area of the materials occurs. Most likely, some thickening of pore walls also takes place (Table 4). After a certain limiting pore size (5.5−6 nm) is reached, the structure of materials starts to disintegrate. The pore size no longer increases, the microporosity develops, and the uniformity of pore structure decreases as evidenced by the appearance of connectivity problems during nitrogen desorption. An excessive hydrothermal treatment leads to materials, which have relatively small pore volumes and surface areas but still exhibit a distinct condensation step in primary mesopores (Figure 7), indicating that there are still some residual uniform pores or groups of pores akin to those of the initial MCM-41 materials.

The current study confirms that the postsynthesis hydrothermal restructuring reported by Khushalani et al.[9] is a convenient way to synthesize high-quality large-pore MCM-41 materials using common surfactants. However, further studies are needed to fully understand the nature of the observed phenomena. It was previously reported[9] that during the hydrothermal process, the surfactant does not undergo decomposition and its molar ratio to silica remains the same, as in the original, nonrestructured materials. It was also shown that water enters the pore space to solvate the silicate framework, the surfactants and their counterions. It is interesting that the adsorption isotherms for the materials (TR1−4d, TR1−5d, and TR1−6d), which underwent an excessive hydrothermal treatment (4−6 days) seem to be similar to the adsorption isotherm for previously described SBA-2[25] sample with 3-D hexagonal structure containing mesoporous cages, which may indicate some degree of similarity of pore structure. As a tentative interpretation, the latter finding may suggest that at some stage of hydrothermal restructuring, the cylindrical micelles of the surfactant may break in some places to form shorter cylindrical or globular micelles (the latter are present in the structure of noncalcined SBA-2). The latter micelles may act as a structure-directing agent during redeposition of silica in the course of the hydrothermal restructuring, which would lead to narrowing of some parts of pores and consequently to the observed poor pore connectivity. Such a scenario would explain the features of the degraded materials, but still the mechanism of the thermal restructuring, especially the initial increase in the pore size, is not well-understood.

The current study shows that the use of both X-ray diffraction and nitrogen adsorption in a wide pressure range is a very powerful tool for probing the textural and structural properties of mesoporous molecular sieves. The application of the high-resolution α_s-plot method appears to be especially promising. The method allows for the assessment of the specific surface area even for samples, which have a considerable amount of small mesopores, for which the nitrogen condensation takes place in the pressure range used in the standard BET method (i.e., between 0.05 and 0.3 p/p_0). The latter phenomenon leads to a high inaccuracy of the BET method.[10] The high-resolution α_s-plot method is also capable of tracing relatively very small amounts of micropores, as shown in the current study for the TR1−2d and TR1−3d samples. Moreover, the method allows us to accurately assess the pore size for MCM-41 materials, especially when X-ray data are available. Therefore, one does not need to apply commonly used methods for pore size calculations, such as BJH[26] or DFT,[27] which may either inadequately reproduce the size of pores (BJH[7]) or provide evidence for nonexisting pores (DFT). The latter problem arises from the fact that the DFT method was developed for carbonaceous materials with slitlike pores. Due to considerable surface and structural differences between graphite slit pores and siliceous cylindrical pores, the DFT method indicates the presence of a significant amount of micropores even for nonmicroporous MCM-41 samples. The problems of pore size and pore size distribution calculations for novel mesoporous materials will be addressed in our forthcoming paper.[28]

CM970128O

(26) Barrett, E. P.; Joyner, L. G.; Halenda, P. P. *J. Am. Chem. Soc.* **1951**, *73*, 373.
(27) Olivier, J. P.; Conkin, W. B.; Szombathely, M. v. In *Characterization of Porous Solids III*; Rouquerol, J., Rodrigues-Reinoso, F., Sing, K. S. W., Unger, K. K., Eds.; Elsevier: Amsterdam, 1994; p 81.
(28) Kruk, M.; Jaroniec, M.; Sayari, A. *Langmuir*, submitted.